

Seismic fragility methodology for highway bridges using a component level approach

Bryant G. Nielson^{1,*} and Reginald DesRoches²

¹*Department of Civil Engineering, Clemson University, Lowry Hall, Clemson, SC 29634-0911, U.S.A.*

²*School of Civil and Environmental Engineering, Georgia Institute of Technology, 790 Atlantic Dr, Atlanta, GA 30332-0355, U.S.A.*

SUMMARY

Bridge fragility curves, which express the probability of a bridge reaching a certain damage state for a given ground motion parameter, play an important role in the overall seismic risk assessment of a transportation network. Current analytical methodologies for generating bridge fragility curves do not adequately account for all major contributing bridge components. Studies have shown that for some bridge types, neglecting to account for all of these components can lead to a misrepresentation of the bridges' overall fragilities.

In this study, an expanded methodology for the generation of analytical fragility curves for highway bridges is presented. This methodology considers the contribution of the major components of the bridge, such as the columns, bearings and abutments, to its overall bridge system fragility. In particular, this methodology utilizes probability tools to directly estimate the bridge system fragility from the individual component fragilities. This is illustrated using a bridge whose construction and configuration are typical to the Central and Southeastern United States and the results are presented and discussed herein. This study shows that the bridge as a system is more fragile than any one of the individual components. Assuming that the columns represent the entire bridge system can result in errors as large as 50% at higher damage states. This provides support to the assertion that multiple bridge components should be considered in the development of bridge fragility curves. The findings also show that estimation of the bridge fragilities by their first-order bounds could result in errors of up to 40%. Copyright © 2006 John Wiley & Sons, Ltd.

Received 6 April 2006; Revised 26 September 2006; Accepted 1 October 2006

KEY WORDS: bridges; seismic; fragility; components; reliability

*Correspondence to: Bryant G. Nielson, Department of Civil Engineering, Clemson University, Lowry Hall, Clemson, SC 29634-0911, U.S.A.

†E-mail: bryant.nielson@ces.clemson.edu

Contract/grant sponsor: National Science Foundation; contract/grant number: EEC-9701785

1. INTRODUCTION

The probabilistic assessment of highway bridges subjected to seismic hazards has developed rapidly over the last two decades. Fragility curves, which are conditional probability statements of a bridge's vulnerability as a function of ground motion intensity, have been a common tool with which we make these seismic assessments. Several methodologies for generating seismic fragility curves for bridges have been developed over the years. The Applied Technology Council (ATC) developed bridge fragility curves based on expert opinion [1]. Empirical methods have also been employed to generate fragility curves for bridges located in California [2] and Japan [3, 4]. Probably, the largest and most diverse fragility generation methodologies are those based on analytical methods. These methods include elastic-spectral [5], non-linear static [6, 7] and non-linear dynamic [8–10] approaches.

Fragility curve methodologies using analytical approaches have become widely adopted because they are more readily applied to bridge types and geographical regions where seismic bridge damage records are insufficient. Because of the lack of strong ground motion records, bridges located in the Central and Southeastern United States (CSUS) are generally assessed using analytical approaches [11]. Most of the analytical bridge fragility studies to date have considered only the bridge columns in vulnerability studies [9, 12, 13]. This simplifying assumption may possibly be appropriate for bridges whose seismic response is largely governed by their columns such as the multiple frame box girder bridge commonly found in California and Japan. However, past research has shown that for bridge types commonly found in the CSUS, having multiple girder supported spans on multi-column bents, all major vulnerable bridge components should be considered to avoid significant errors in the estimation of bridge fragilities [14]. Recognition of this issue resulted in a study where several bridge components were considered in developing system (bridge) level fragility curves [8]. This study estimated the system level fragility curves using first-order reliability bounds and conservatively assumed that the upper bound represented the system fragility.

The purpose of this paper is to present a more direct approach for estimating system level fragility curves while accounting for the vulnerability contribution of various bridge components. The proposed fragility curve methodology eliminates the need to rely on system fragility bounds and their associated restriction to serial systems. This methodology, which utilizes time history analyses, is illustrated in detail for a bridge type common to the CSUS. Specifically, 3-D analytical models are used to incorporate the impact of excitation orientation and also the effects of various bridge components in both the transverse and longitudinal directions.

2. METHODOLOGY

Fragility theory is a generalized branch of structural reliability which assesses the vulnerability of a structure conditioned upon some other input parameter. For seismic loading, the fragility simply looks at the probability that the seismic demand placed on the structure (D) is greater than the capacity of the structure (C). This probability statement is conditioned on a chosen intensity measure (IM) which represents the level of seismic loading. The generic representation of this conditional probability is given as

$$\text{Fragility} = P[D \geq C | \text{IM}] = P[C - D \leq 0.0 | \text{IM}] \quad (1)$$

Evaluation of Equation (1) is most easily accomplished by developing a probability distribution for the demand conditioned on the IM, also known as a probabilistic seismic demand model (PSDM), and convolving it with a distribution for the capacity. The demand on the structure is quantified using some chosen metric(s) (e.g. deformation, ductility). Cornell *et al.* [15] suggested that the estimate for the median demand (S_d) can be represented by a power model as

$$S_d = aIM^b \quad (2)$$

where IM is the seismic intensity measure of choice and both a and b are regression coefficients. Furthermore, the distribution of the demand about its median is often assumed to follow a two parameter lognormal probability distribution [15, 16]. Thus, after estimating the dispersion ($\beta_{D|IM}$) of the demand about its median, which is conditioned upon the IM, the PSDM may be written as shown

$$P[D \geq d | IM] = 1 - \Phi \left(\frac{\ln(d) - \ln(aIM^b)}{\beta_{D|IM}} \right) \quad (3)$$

The generation of the PSDMs in this study follows the procedure as outlined below.

1. Assemble a suite of N ground motions which are applicable to the geographical area of interest. This suite should represent a broad range of values for the chosen intensity measure.
2. Generate N statistical samples of the subject structure. These samples should be generated by sampling on various modelling parameters which may be deemed significant (e.g. damping ratio and material strengths). Thus, N statistically different yet nominally identical bridge samples are generated.
3. Perform a full non-linear time history analysis for each ground motion–bridge pair. Key responses should be monitored throughout the analysis.
4. For each analysis, peak responses are recorded and plotted *versus* the peak value of the intensity measure for that ground motion. A regression analysis of these data are then performed to estimate a , b and $\beta_{D|IM}$.

Step 4 is repeated for all major vulnerable components in the bridge. Thus, the seismic demand on each of the bridge components may be modelled.

The seismic capacity of a bridge component refers to a level at which the bridge loses some measure of functionality. Often, capacity is thought of as the level beyond which the structure collapses. However, in this study, the capacity can be chosen as any level which is of interest to the analyst. For instance, one may assess that a deformation of 25 mm in a bearing will result in the bridge being closed to traffic for one day while the bridge is jacked back into place. However, a deformation of 200 mm might be assumed as a level that will cause collapse of the bridge span and result in a closure of >180 days.

The capacity levels (limit states) for the various bridge components may be assessed using a physics (prescriptive) approach [10] and/or a judgemental (descriptive) approach [17]. A physics-based approach examines the mechanics of the problem and prescribes some functional level to be assigned to the bridge for various levels of damage. This is usually the preferred method but it requires some level of engineering analysis. A judgemental approach tries to capture or describe the functionality levels which would be assigned to the bridge by decision makers (bridge inspectors) for different levels of observed damage. Although this is a more subjective approach, post-damage bridge functionality is generally assigned in this manner.

In this study, the distributions of the component capacities are assumed to be lognormal. The lognormal parameters for limit states (S_c , β_c) of each bridge component used are subsequently developed using a Bayesian approach that incorporates physics-based assessments with judgemental assessments. This is more specifically addressed in the case study presented later in this paper.

Since the demand and capacity of the structural components are all assumed to follow lognormal distributions, the fragility statement in Equation (1) will take the following form:

$$P[D > C | IM] = \Phi \left[\frac{\ln(S_d/S_c)}{\sqrt{\beta_{D|IM}^2 + \beta_c^2}} \right] \quad (4)$$

where S_d is the median estimate of the demand, S_c is the median estimate of the capacity, $\beta_{D|IM}$ is the dispersion or logarithmic standard deviation of the demand conditioned on the intensity measure and β_c is the dispersion of the capacity. In this manner, the fragility curves for each of the bridge components are developed.

The general assessment of seismic vulnerability for the bridge (system) as a whole must be made by combining the effects of the various bridge components. The probability that the bridge is at or beyond a particular limit state ($\text{Fail}_{\text{system}}$) is the union of the probabilities of each of the components being in that same limit state ($\text{Fail}_{\text{component}-i}$), as shown in the following:

$$P[\text{Fail}_{\text{system}}] = \bigcup_{i=1}^n P[\text{Fail}_{\text{component}-i}] \quad (5)$$

The estimate of the system or bridge level fragility is facilitated through the development of a joint probabilistic seismic demand model (JPSDM). This approach is in recognition that there is some level of correlation between the demands placed on the various bridge components during a given earthquake. Thus, the seismic demand on the system is simply the joint demand on the components. As previously stated, the demands on the components are assumed to follow lognormal distributions. Therefore, the natural logarithm of the demands, shown in Equation (6), must follow a jointly normal distribution as

$$\ln(S_d) = \ln(a) + b \ln(IM) \quad (6)$$

The JPSDM is developed in this transformed state by using the transformed marginal distributions of the individual components and developing the covariance matrix through estimation of the correlation coefficients between the transformed demands. Using the capacity models and the JPSDM, Equation (5) can be evaluated using a Monte Carlo simulation. Evaluation is done for various levels of the IM resulting in a probability of 'failure' of the system at each level. The parameters for the system level fragility curve are then estimated using regression analysis.

The method presented here looks at multiple bridge components as possible sources of failure. As illustrated, the basic framework of the methodology presented in this study is commonly used in the fragility assessment of highway bridges. However, the key improvement is the use of a JPSDM for including the effects of multiple bridge components. By developing the JPSDM, the system fragility can be directly estimated rather than using system bounds as has been done in previous studies [8]. It should be noted that the specifics on the application of this methodology will vary depending on the type of bridge being considered. For example, the number and type of bridge components to consider may vary from one bridge type to another. Also, the capacity models used for one type of bridge may not be appropriate for another type.

3. CASE STUDY

The methodology for the generation of seismic fragility curves, as presented in the previous section, is illustrated using a class of highway bridges common to the CSUS. The selected bridge type is a multi-span simply supported (MSSS) concrete girder bridge. A detailed review of the concrete girder bridges in the national bridge inventory (NBI) shows that the MSSS concrete girder bridges account for approximately 19% of the highway bridges which is the single largest bridge class the region [18]. This case study develops generalized fragility curves for this class of bridges and not for a specific bridge.

3.1. Bridge description and modelling

Over 81% of the MSSS concrete girder bridges were built prior to 1990, which is indicative of limited seismic detailing and their relatively small use in current construction. To give an idea of typical geometric properties of this bridge class, empirical cumulative distribution functions (CDFs) are generated and shown in Figure 1. The span lengths for over 90% of this bridge type fall in the range of 6–25 m. The 90th percentile for the deck widths and column heights are around 13 and 7 m, respectively. The most likely number of spans is three with a probability of 42% and over 83% of all bridges fall in the range of 2–5 spans. The skew is 0° for over 70% of the bridges and over 86% of all the bridges have a skew which is less than 30° .

By sampling on the information from the inventory analysis, eight representative (not actual) bridge configurations are defined. These sample bridges have three spans with 0° skew and have the geometric properties listed in Table I. Figure 2 presents the generic layout of this bridge type.

Details for this bridge type are taken from bridge plans for several existing bridges located in Memphis, TN. The appropriateness of applying these details to the general class of MSSS concrete girder bridges is justified in previous studies [19, 20]. These bridges generally use multi-column bents which are founded on driven pile foundations with eight piles under each footing. The bridge ends are supported by pile-bent abutments. The superstructure is constructed of concrete girders and a concrete deck. These bridges typically use elastomeric pads for bearings. Steel dowels are placed in the top of the bent beam and extend into the underside of the concrete girders to act as

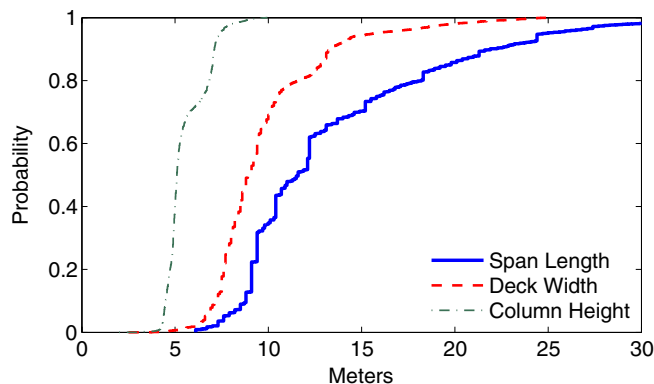


Figure 1. Empirical cumulative distribution functions for geometric properties of MSSS concrete girder bridge class.

Table I. Geometric configurations for eight representative bridges.

Bridge no.	Spans	Middle span length (m)	End span lengths (m)	Deck width (m)	Column height (m)
1	3	7.6	7.6	9.5	4.4
2	3	9.1	9.1	9.5	3.3
3	3	10.7	10.7	15.2	3.7
4	3	20.1	12.2	9.5	4.0
5	3	13.4	12.2	9.5	4.2
6	3	9.4	9.4	9.5	6.0
7	3	12.2	12.2	20.9	6.1
8	3	27.4	12.2	9.5	3.9

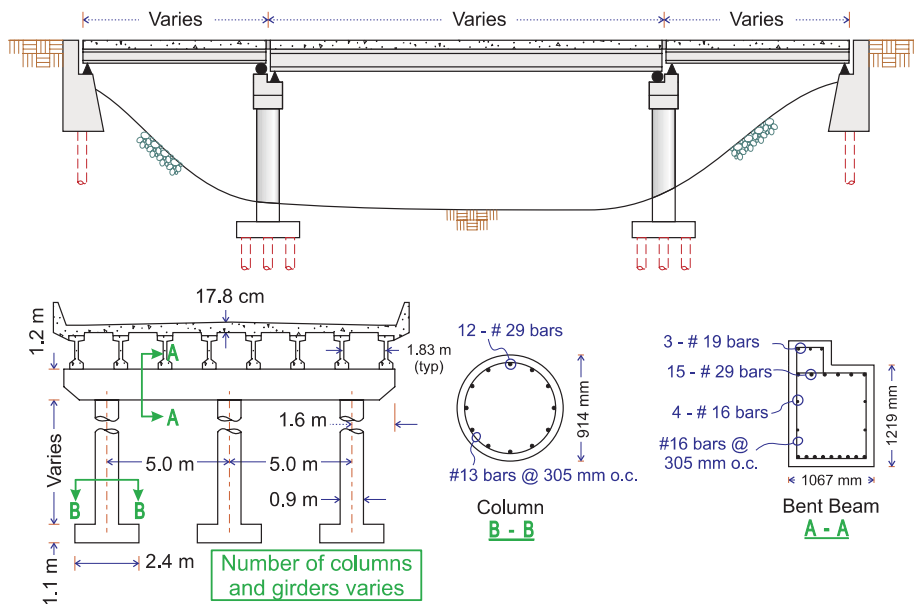


Figure 2. General configuration of MSSS concrete girder bridge class.

girder restraint devices. Expansion in the deck is accommodated by providing slotted holes in one end of the girder.

Using the OpenSees analysis platform [21], detailed non-linear 3-D models are created for each subject bridge. A brief description of the analytical modelling procedure is given in this paper. However, for a full treatment of the analytical models see the work by Nielson [18].

The superstructure, which refers to the composite slab and girder section, is expected to remain linear and is thus modelled using linear elastic beam-column elements. Pounding between the decks is accounted for using the contact element approach including the effects of hysteretic energy loss which is outlined in the work by Muthukumar and DesRoches [22]. Damping is accounted for in the model using Rayleigh damping but is treated as a random variable (see Table II).

Table II. Uncertainty incorporated in analytical bridge models.

Modelling parameter	Probability distribution	Distribution parameters		Units
		1	2	
Steel strength	Lognormal	$\lambda = 6.13$	$\zeta = 0.08$	MPa
Concrete strength	Normal	$\mu = 33.8$	$\sigma = 4.3$	MPa
Bearing shear modulus	Uniform	$l = 0.66$	$u = 2.07$	MPa
Bearing coefficient of friction	Lognormal	$\lambda = \ln(\text{med})^*$	$\zeta = 0.1$	
Passive stiff of abutments	Uniform	$l = 11.5$	$u = 28.8$	kN/mm/m
Active stiffness of abutments	Uniform	$l = 2.2$	$u = 6.6$	kN/mm/m
Translational foundation stiff	Uniform	$l = 28$	$u = 84$	kN/mm/ftg
Rotational foundation stiff	Uniform	$l = 3.03(10)^5$	$u = 9.09(10)^5$	kN m/rad
Deck mass	Uniform	$l = 0.9^\dagger$	$u = 1.1$	
Damping ratio	Normal	$\mu = 0.045$	$\sigma = 0.0125$	
Internal hinge gaps	Normal	$\mu = 25.4$	$\sigma = 3.3$	mm
Abutment–deck gaps	Normal	$\mu = 38.1$	$\sigma = 1.01$	mm
Loading direction	Uniform	$l = 0$	$u = 2\pi$	radians

*Bearing friction is a function of the normal stress placed on the bearing. The median value for the distribution is assumed to be the same as the value calculated as per [23].

†Distribution for deck mass is uniformly distributed from 90 to 110% of the calculated deck mass.

The columns are modelled using non-linear beam–column elements whose cross-section is defined using fibres. Each fibre of the cross-section is modelled with an appropriate stress–strain relationship depending on whether it represents confined concrete, unconfined concrete or longitudinal reinforcing steel. The bent beams are modelled using the same type of elements as used for the columns and are assumed to be rectangular.

The bearings are modelled using non-linear translational springs which account for the contribution of the elastomeric pads in addition to the effect of the steel dowels. The elastomeric pads are modelled with an elastic perfectly plastic material where the initial stiffness is calculated using the geometry of the pad.

The behaviour of the abutments is incorporated in the model through the use of non-linear translational springs. The stiffnesses of the abutment springs are a function of the passive resistance of the soil and also the stiffness of the piles. Spring constants are calculated based on the recommendation of Caltrans [24]. The constants for the translational and rotational springs for the pile foundations were found in a similar manner.

3.2. Ground motion suite

The seismic response of this bridge is evaluated using a suite of synthetic ground motions developed as a part of the on-going research in the Mid-America Earthquake (MAE) Center. Rix and Fernandez-Leon [25] generated a suite of deterministic ground motions for Memphis, TN which consider the effects of source, path and site. The suites were generated for three different moment magnitudes M_w (5.5, 6.5 and 7.5) and four different hypocentral distances (10, 20, 50 and 100 km). The ground motions were developed for a soil profile typical to Memphis, TN where sediments in the Mississippi embayment are of concern. Of the original 220 ground motions generated, 48 were selected for use in this study. Time histories were selected from each of the

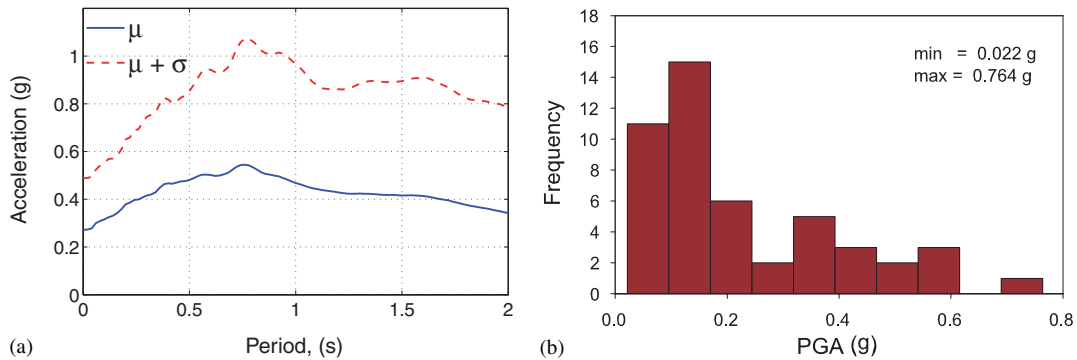


Figure 3. (a) Mean and mean plus one standard deviation acceleration response spectra; and (b) histogram of PGA values for selected ground motion suite.

magnitude–distance bins to create the suite of 48. This was done to ensure that the assembled suite had frequency content (Figure 3(a)) representative of both large and small earthquakes with varying distances. Ground motions selected from each bin were those with the largest values of peak ground acceleration (PGA) to ensure a broad range of PGA values (see Figure 3(b)) that would induce non-linear response in the bridges. The ground motions were then split into orthogonal components facilitating the 3-D analysis [18]. Vertical ground motions were not considered for this study since previous studies have shown that they are not necessary for analysis of bridges in the CSUS [26].

3.3. Probabilistic seismic demand models

Prior to the generation of the PSDMs, the statistical samples of the bridge must be generated. Random samples of various modelling parameters are combined with the eight geometric bridge samples given in Table I to give 48 bridge models. A Latin-hypercube sampling [27], which is a variance reduction sampling technique, was used to generate these bridge models. This sampling is performed to account for the epistemic uncertainty in the bridge inventory as it applies to geometry, material properties, component behaviours and damping. Table II presents the modelling parameters and the probability distributions used to model them. Many of the distributions and values assigned to the various modelling parameters are pulled from the literature, including steel strength [28], concrete strength [29], bearing friction [30], damping ratio [31, 32] and deck gaps [19]. For the other modelling parameters, published distribution information is not available. Therefore, to account for some degree of uncertainty, uniform distributions were assigned to these parameters where the lower and upper levels are 50% and 150% of the calculated deterministic values.

The 48 bridge models are paired with the 48 synthetic ground motions and are analysed using non-linear time history analyses. During the analyses, eight different component responses are monitored and recorded which are inclusive of bridge components historically damaged in earthquakes. Specifically, the component responses are column curvature ductility (μ_ϕ), longitudinal and transverse deformation (δ , mm) in the fixed bearings, longitudinal and transverse deformation (δ , mm) in the expansion bearings and active, passive and transverse deformation (δ , mm) in the abutments. Peak ground acceleration (PGA) is selected for the conditioning

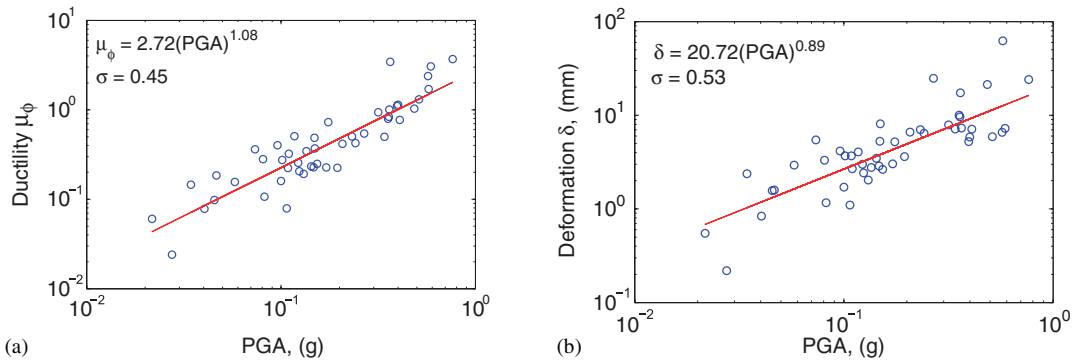


Figure 4. Probabilistic seismic demand models for: (a) columns; and (b) abutments.

Table III. Probabilistic seismic demand models in transformed state for eight component responses.

Response	PSDM	R ²	(β _{D PGA})
ln(μ _φ)	ln(2.72) + 1.08 * ln(PGA)	0.82	0.45
ln(f _{xL})	ln(57.23) + 1.06 * ln(PGA)	0.66	0.66
ln(f _{xT})	ln(6.69) + 0.30 * ln(PGA)	0.55	0.23
ln(e _{xL})	ln(108.00) + 1.01 * ln(PGA)	0.76	0.50
ln(e _{xT})	ln(10.86) + 0.50 * ln(PGA)	0.39	0.55
ln(ab _P)	ln(18.16) + 1.174 * ln(PGA)	0.79	0.53
ln(ab _A)	ln(20.72) + 0.89 * ln(PGA)	0.68	0.53
ln(ab _T)	ln(11.76) + 1.02 * ln(PGA)	0.73	0.54

intensity measure as it has been shown to be a good intensity measure when dealing with bridge classes [33]. Figure 4 illustrates the maximum seismic demands placed on the (a) columns and the (b) abutments in the active action. This figure also illustrates the estimate for the median demand and conditional dispersion for each component. When plotted in log–log space the line representing the estimate for the median demand appears as a straight line. One should note that the number of ground motions (samples) used in the simulation has a direct effect on the confidence bands associated with the median demand. The confidence level in this estimate increases as the number of simulations increases. However, the analyst must balance the desired confidence level with the computational expense associated with each simulation. In this study, 48 simulations are assumed to be adequate to illustrate the methodology presented.

The JPSDM is developed by first taking the natural logarithm of each of the eight monitored component responses. In this transformed state, the PSDM is written as shown in Table III, which presents the median estimates (PSDM) and dispersion estimates (β_{D|PGA}) of the demand for all eight responses. The correlation coefficients between the demands in the transformed state are estimated and presented in Table IV. The marginals and correlation coefficients fully define the jointly normal distribution in the transformed state.

Table IV. Correlation coefficients between the natural log of eight component responses.

	$\ln(\mu_\varphi)$	$\ln(f_{x_L})$	$\ln(f_{x_T})$	$\ln(ex_L)$	$\ln(ex_T)$	$\ln(ab_P)$	$\ln(ab_A)$	$\ln(ab_T)$
$\ln(\mu_\varphi)$	1.00	0.86	0.63	0.97	0.66	0.95	0.84	0.87
$\ln(f_{x_L})$	0.86	1.00	0.68	0.86	0.71	0.88	0.65	0.75
$\ln(f_{x_T})$	0.63	0.68	1.00	0.64	0.98	0.69	0.44	0.63
$\ln(ex_L)$	0.97	0.86	0.64	1.00	0.68	0.93	0.81	0.83
$\ln(ex_T)$	0.66	0.71	0.98	0.68	1.00	0.72	0.42	0.63
$\ln(ab_P)$	0.95	0.88	0.69	0.93	0.72	1.00	0.81	0.86
$\ln(ab_A)$	0.84	0.65	0.44	0.81	0.42	0.81	1.00	0.82
$\ln(ab_T)$	0.87	0.75	0.63	0.83	0.63	0.86	0.82	1.00

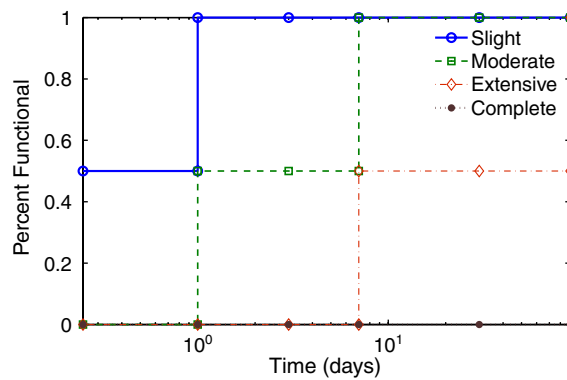


Figure 5. Bridge functionality restoration curves used for definition of quantitative limit states as derived from damage functionality survey.

3.4. Limit state models

The capacities of the bridge components are defined in terms of limit state models. Traditionally, these limit states for bridge components have been defined by qualitative damage states such as slight, moderate, extensive and complete [34]. Associated with each of these damage states is a timeline for the restoration of the bridge functionality. This restoration timeline is essential for the portability of the bridge fragility models in loss assessment packages such as HAZUS-MH [34]. For the purposes of this study, the four damage states previously listed are used and the associated restoration curves are given in Figure 5. Note that the restoration curves are step functions with possible values of 0, 50 and 100% operability as a function of post-event time. This timeline was selected to closely resemble the restoration timelines in HAZUS-MH.

With the definition of qualitative damage states, quantitative limit states must be derived. These limit states should use the same metrics as were used for the PSDMs. As previously stated, there are two general approaches for defining these limit states. One method takes a physics-based approach and the other takes a descriptive approach. Recognizing that both approaches have valid arguments for usage, a Bayesian approach is used to incorporate the information from both approaches. The median values of the prescriptive limit states previously used in the work by Choi [19] are used in this study. A coefficient of variation (COV) of 0.25, 0.25, 0.46 and 0.46 is assigned to slight,

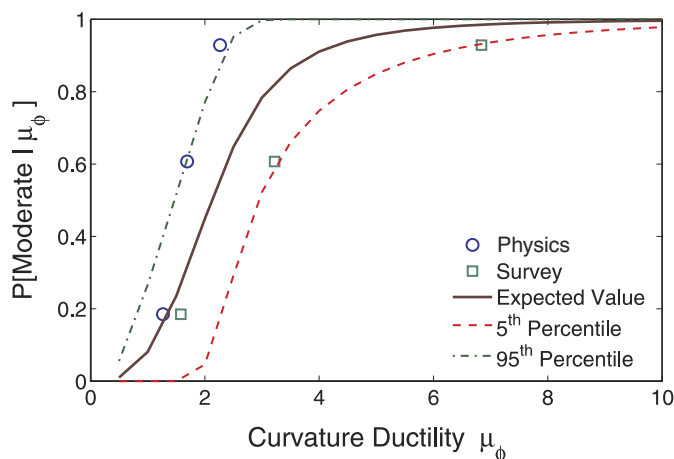


Figure 6. Bayesian updating of distributions of moderate damage state for columns.

moderate, extensive and complete damage states, respectively. These COVs recognize that there is more aleatoric uncertainty present in the higher damage states.

The definition of the descriptive limit states are derived from the work by Padgett and DesRoches [35]. In their study, they surveyed bridge inspectors and engineers working in CSUS departments of transportation about the closure decisions given for various levels of damage. These queries specifically looked at bridge closure decisions as a function of time. This information was used to generate percentile estimates for closure times based on observed damage. The derivation of these limit states is beyond the scope of this paper but a full treatment can be found in [18]. One interesting phenomenon is that there was considerably more uncertainty in the lower damage states when compared with the higher damage states. It appears that decision makers were more uncertain on closure decisions for small occurrences of damage.

Using a Bayesian approach, the limit states used in this study are a combination of both the prescriptive and the descriptive limit states. Following the work of Mosleh and Apostolakis [36], the previously mentioned prescriptive limit states were updated with the results from the survey. Figure 6 illustrates the implementation of this Bayesian updating for the moderate damage state of the columns. The resulting limit states for all considered components are given in Table V which represent the expected distributions as seen in Figure 6. The median values for column curvature ductility are unitless and are presented as such. The median values for the bearings and abutments are reported in millimeters which is consistent with the metric used to quantify demand. The limit states for both fixed and expansion bearings are assumed to be the same in this study.

3.5. Component fragility curves

Fragility curves for each of the bridge components are easily calculated using the marginal distributions of the JPSDM and the capacity limit states in the framework of Equation (4). The resulting component fragility curves follow a lognormal distribution with median values (expressed in terms of g) and dispersion values as given in Table VI. Figure 7 plots the fragility curves for the bridge components for the slight and moderate damage states. For clarity, the transverse bearings have not been included in Figure 7 because of their high median values (See Table VI).

Table V. Medians and dispersions for bridge component limit states using Bayesian updating.

Component	Slight		Moderate		Extensive		Complete	
	Median	Dispersion	Median	Dispersion	Median	Dispersion	Median	Dispersion
Column (μ_ϕ)	1.29	0.59	2.10	0.51	3.52	0.64	5.24	0.65
Elastomeric bearing—long (mm)	28.9	0.60	104.2	0.55	136.1	0.59	186.6	0.65
Elastomeric bearing—trans (mm)	28.8	0.79	90.9	0.68	142.2	0.73	195.0	0.66
Abut—passive (mm)	37.0	0.46	146.0	0.46	N/A	N/A	N/A	N/A
Abut—active (mm)	9.8	0.70	37.9	0.90	77.2	0.85	N/A	N/A
Abut—trans (mm)	9.8	0.70	37.9	0.90	77.2	0.85	N/A	N/A

Table VI. Medians and dispersions for bridge component fragilities at four damage states.

Component	Slight		Moderate		Extensive		Complete	
	Median (g)	Dispersion	Median (g)	Dispersion	Median (g)	Dispersion	Median (g)	Dispersion
Column	0.50	0.69	0.79	0.63	1.27	0.72	1.84	0.73
Fxd elastomeric Bearing—long	0.52	0.85	1.76	0.81	2.27	0.84	3.07	0.88
Fxd elastomeric Bearing—trans	99.00*	N/A	99.0*	N/A	99.0*	N/A	99.0*	N/A
Exp elastomeric Bearing—long	0.27	0.78	0.97	0.73	1.26	0.76	1.72	0.81
Exp elastomeric Bearing—trans	99.0*	N/A	99.0*	N/A	99.0*	N/A	99.0*	N/A
Abut—passive	1.83	0.60	99.0*	N/A	99.0*	N/A	99.0*	N/A
Abut—active	0.43	0.98	1.97	1.18	99.0*	N/A	99.0*	N/A
Abut—trans	0.83	0.86	3.14	1.03	99.0*	N/A	99.0*	N/A

*Estimated median values are much larger than can be appropriately extrapolated from regression analyses. Thus, median values of 99.0 imply unknown yet high median values.

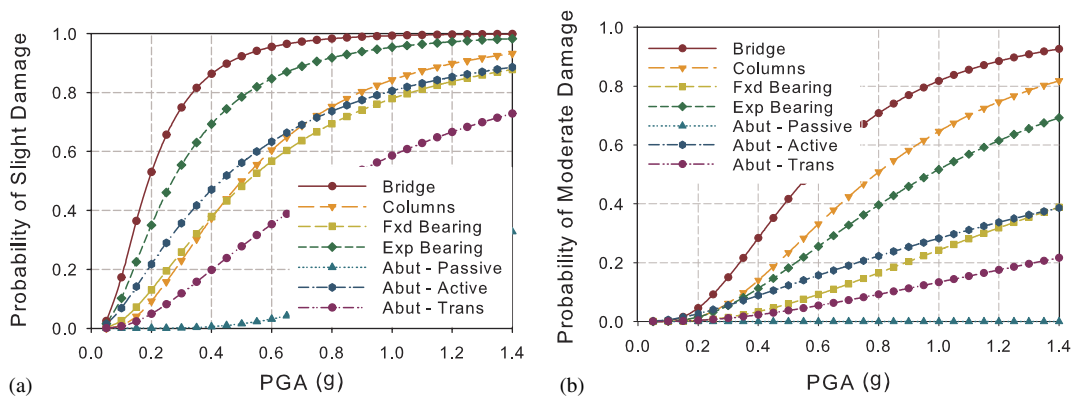


Figure 7. Bridge and component fragility curves for: (a) slight damage; and (b) moderate damage.

The abutments and expansion bearings appear to be the most fragile components in the slight damage state while the columns and expansion bearings are most fragile for moderate damage. The primary reason for the shift in the most fragile components is clearly seen in Table V. There is not a consistent difference between the median values of the component limit states. For instance, the median value for the abutment in active action at the moderate damage level is approximately 300% higher than its value for slight damage (similar for expansion bearings). This same increase is reduced to approximately 60% when considering the columns. Therefore, one may see that while the columns are the third most fragile component when considering slight damage, they become the most fragile component when considering moderate damage. One should recall that the limit state values are strongly influenced by the survey responses of bridge inspectors and engineers and are thus indicative of perceived impacts of various damage levels on bridge functionality.

3.6. System fragility curves

The fragility curve generation for the entire bridge utilizes the JPSDM and the limit state models in a crude Monte Carlo simulation which does not include variance reduction sampling. This simulation is intended to integrate the JPSDM over all possible failure domains. This is done by selecting a value of the IM, which in this case is PGA. At this level of IM, $(10)^6$ samples are taken from both the demand and capacity sides. Next, an estimate of the probability that the demand exceeds the capacity at that IM level is obtained. This step is repeated for increasing levels of the IM until a curve is defined. Median values for slight, moderate, extensive and complete damage of the bridge system are calculated as 0.19, 0.57, 0.83 and 1.18g, respectively. The dispersions for each damage state are approximately the same, ranging from 0.62 to 0.68.

In addition to the fragility curves for each of the bridge components, the bridge system fragility curves are also plotted in Figure 7. Clearly, the bridge as a system is more fragile than any one of the bridge components. One would expect that using a single demand indicator (e.g. column ductility) would result in an underestimation of a bridge's seismic vulnerability. This may be particularly true for MSSS bridges which are highly susceptible to excessive deformation in the bearings and subsequent unseating of the decks.

As shown in this case study, the value of the median for the slight damage state for the columns is 0.50g. The value for the median of the slight damage state of the entire bridge system is 0.19g producing a difference of over 160%. The differences between the median values of the system and column fragilities at the higher damage states are smaller. These differences, as shown in Table VII, are in the range of 35–55%. The reason for this observed phenomenon is best illustrated considering Equation (7) which defines the bounds on the system. When only

Table VII. Median values for the fragility curves of the bridge system, its upper and lower bounds and also for its columns.

Damage state	Bridge	Upper bound		Lower bound		Columns only	
	Median (g)	Median (g)	Difference (%)	Median (g)	Difference (%)	Median (g)	Difference (%)
Slight	0.19	0.17	11	0.27	42	0.50	163
Moderate	0.57	0.49	14	0.78	37	0.79	36
Extensive	0.83	0.78	6	1.26	52	1.27	53
Complete	1.18	1.05	11	1.72	46	1.84	56

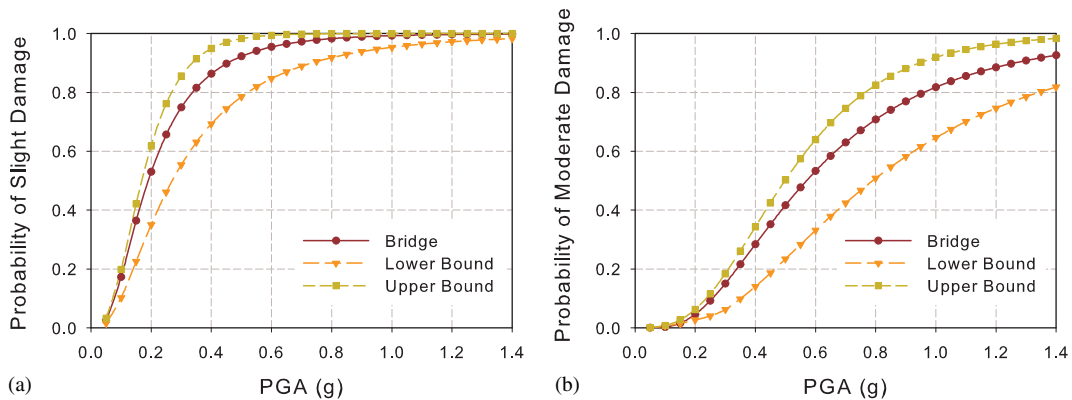


Figure 8. Bridge and system fragility bounds for: (a) slight damage; and (b) moderate damage.

one component significantly contributes to the system fragility the bounds become very narrow (small difference). Conversely, when many components contribute, the bounds become wider. In this study, many components contribute to slight damage—creating large differences between the system and any single component—while only two significantly contribute to complete damage which tends to lower this discrepancy (see Table VI). Clearly, one may deduce that fragilities developed considering just the vulnerability of a single component (e.g. columns) would not be appropriate for this particular bridge type.

One option for assessing the fragility of the overall bridge system is to calculate the upper and lower first-order bounds on the system. For a serial system, this is typically done by collecting the fragilities of each of the bridge components and implementing them into the following equation:

$$\max_{i=1}^n [P(F_i)] \leq P(F_{\text{system}}) \leq 1 - \prod_{i=1}^m [1 - P(F_i)] \quad (7)$$

where $P(F_i)$ is the probability of failure of component i and $P(F_{\text{system}})$ is the probability of the system. The maximum of the component fragilities is considered to be the lower and consequently unconservative bound. This bound assumes that the demands on the bridge components are completely correlated. What follows is that the upper bound (conservative) assumes no correlation between the component demands. Figure 8 compares the system bounds with those calculated for the slight and moderate damage states using the methodology presented in this study. As seen in this figure, the bridge system fragilities lie closer to the upper bound which is what one would expect given the relatively high correlation values shown in Table IV. Table VII presents the median values for the system, upper and lower bounds. This table also shows the percentage difference between the medians of the bridge system and the medians of the bounds. There is approximately a 10% difference between the upper bound medians and the directly calculated medians. This difference is much larger between the bridge and the lower bound which is around 45%. These differences illustrate that if a system bound is used as an approximation to the system fragility that the conservative upper bound would be a more appropriate selection as was done in previous studies [8]. As previously stated, this conclusion is also reinforced by the high level of correlation as shown in Table IV. However, the 10% error associated with using this bounding estimate of the system fragility can be eliminated by using the more direct approach presented herein.

4. CONCLUSIONS

This study presents an analytical methodology for developing seismic fragility curves for highway bridges. Specifically, this methodology is designed to provide consideration of all major bridge components in assessing seismic vulnerabilities. The demand on the bridge is quantified by using a JPSDM. The fragility of the bridge is calculated by integrating over all failure domains of the joint PSDM. Probabilistic models for the capacities are assumed to be lognormal and are used to define the failure domains of the JPSDM.

A case study illustrating this technique of directly calculating seismic bridge system fragility curves is presented for a MSSS concrete girder class of bridges. The subject bridge class is represented by a suite of 3-D analytical models which are subjected to a suite of synthetic ground motions. The results from these analyses are then used to generate the joint PSDM needed by the proposed methodology. The bridge components considered in the development of this joint PSDM include the columns, bearings and abutments. Once the PSDM is defined, along with appropriate capacity models, the fragility models for this particular bridge could be calculated.

The resulting fragility curves for both the bridge components and the bridge system as a whole show that the bridge system is more fragile than any one of the bridge components. For the slight damage state the expansion bearings are calculated to be the most fragile with a median value of 0.27g. The bridge system for the same damage state is calculated to be 0.19g showing a difference of 42%. For the moderate damage state the columns are seen to be the most fragile of the components with a median value of 0.79g. This compares with the system fragility having a median of 0.57g and a resulting error of 39%. This illustrates that using the fragility of any single bridge component to represent the overall vulnerability of the bridge would likely result in a significant underestimation of that vulnerability.

First-order bounds on the system fragility curves were also developed to provide comparison with the fragilities calculated using the direct estimation procedure presented in this study. The largest discrepancies occurred between the directly calculated fragilities and lower bound estimates. Errors resulting from using the lower bound as the estimate of the system fragility are greater than 40%. The errors between the system fragilities and their upper bounds are approximately 10%. The analysis presented in this study, has considerable epistemic and aleatoric uncertainty associated with it. The methodology presented in this paper is relatively straightforward in its implementation and is an effective means of decreasing the epistemic uncertainty in the analysis.

ACKNOWLEDGEMENTS

This study has been supported by the Earthquake Engineering Research Center program of the National Science Foundation under Award Number EEC-9701785 (Mid-America Earthquake Center).

REFERENCES

1. ATC. Earthquake damage evaluation data for California. *ATC-13*. Applied Technology Council, 1985.
2. Basoz N, Kiremidjian AS. Development of empirical fragility curves for bridges. *5th US Conference on Lifeline Earthquake Engineering*, ASCE: Seattle, WA, U.S.A., 1999.
3. Shinozuka M, Feng MQ, Lee J, Naganuma T. Statistical analysis of fragility curves. *Journal of Engineering Mechanics* 2000; **126**:1224–1231.
4. Yamazaki F, Hamada T, Motoyama H, Yamauchi H. Earthquake damage assessment of expressway bridges in Japan. *Technical Council on Lifeline Earthquake Engineering Monograph* 1999; 361–370.

5. Jernigan JB, Hwang H. Development of bridge fragility curves. *7th US National Conference on Earthquake Engineering*, EERI: Boston, MA, 2002.
6. Mander JB, Basoz N. Seismic fragility curve theory for highway bridges. *5th US Conference on Lifeline Earthquake Engineering*. ASCE: Seattle, WA, U.S.A., 1999.
7. Monti G, Nistico N. Simple probability-based assessment of bridges under scenario earthquakes. *Journal of Bridge Engineering* 2002; **7**:104–114.
8. Choi E, DesRoches R, Nielson B. Seismic fragility of typical bridges in moderate seismic zones. *Engineering Structures* 2004; **26**:187–199.
9. Karim KR, Yamazaki F. A simplified method of constructing fragility curves for highway bridges. *Earthquake Engineering and Structural Dynamics* 2003; **32**:1603–1626.
10. Mackie KR, Stojadinovic B. Post-earthquake functionality of highway overpass bridges. *Earthquake Engineering and Structural Dynamics* 2006; **35**:77–93.
11. Hwang H, Jernigan JB, Lin Y-W. Evaluation of seismic damage to Memphis bridges and highway systems. *Journal of Bridge Engineering* 2000; **5**:322–330.
12. Mackie K, Stojadinovic B. Fragility curves for reinforced concrete highway overpass bridges. *13th World Conference on Earthquake Engineering*, Vancouver, BC, Canada, 2004.
13. Shinozuka M, Feng MQ, Kim H-K, Kim S-H. Nonlinear static procedure for fragility curve development. *Journal of Engineering Mechanics* 2000; **126**:1287–1296.
14. Nielson BG, DesRoches R. Improved methodology for generation of analytical fragility curves for highway bridges. *9th ASCE Specialty Conference on Probabilistic Mechanics and Structural Reliability*. ASCE: Albuquerque, NM, 2004.
15. Cornell AC, Jalayer F, Hamburger RO. Probabilistic basis for 2000 SAC federal emergency management agency steel moment frame guidelines. *Journal of Structural Engineering* 2002; **128**:526–532.
16. Song J, Ellingwood BR. Seismic reliability of special moment steel frames with welded connections: II. *Journal of Structural Engineering* 1999; **125**:372–384.
17. Hwang H, Jernigan JB, Billings S, Werner SD. Expert opinion survey on bridge repair strategy and traffic impact. *Post Earthquake Highway Response and Recovery Seminar*. CERl: St. Louis, MO, 2000.
18. Nielson BG. Analytical fragility curves for highway bridges in moderate seismic zones. *Ph.D. Thesis*, Georgia Institute of Technology, 2005.
19. Choi E. Seismic analysis and retrofit of mid-America bridges. *Ph.D. Thesis*, Georgia Institute of Technology, 2002.
20. Hwang H, Liu JB, Chiu Y-H. Seismic fragility analysis of highway bridges. *MAEC RR-4*, Center for Earthquake Research Information, 2000.
21. McKenna F, Feneves GL. *Open System for Earthquake Engineering Simulation Pacific Earthquake Engineering Research Center, Version 1.6.2*, Pacific Earthquake Engineering Research Center, 2005.
22. Muthukumar S, DesRoches R. A Hertz contact model with non-linear damping for pounding simulation. *Earthquake Engineering and Structural Dynamics* 2006; **35**:811–828.
23. Schrage I. Anchoring of bearings by friction. *Joint Sealing and Bearing Systems for Concrete Structures, World Congress on Joints and Bearings*, American Concrete Institute, Niagara Falls, NY, U.S.A., 1981.
24. Caltrans. *Caltrans Seismic Design Criteria* (2nd edn). California Department of Transportation: Sacramento, CA, 1999.
25. Rix GJ, Fernandez-Leon JA. *Synthetic Ground Motions for Memphis*, TN, 2004 [cited July 2, 2004]; Available from: http://www.ce.gatech.edu/research/mae_ground_motion
26. ATC/MCEER. Recommended LRFD guidelines for the seismic design of highway bridges, Part I: Specifications. *MCEER/ATC-49*. Applied Technology Council and Multidisciplinary Center for Earthquake Engineering Research Center, 2003.
27. Ayyub BM, Lai K-L. Structural reliability assessment using latin hypercube sampling. *Proceedings of ICOSSAR'89, the 5th International Conference on Structural Safety and Reliability, Part II*. ASCE: San Francisco, CA, U.S.A., 1989.
28. Ellingwood B, Hwang H. Probabilistic descriptions of resistance of safety-related structures in nuclear plants. *Nuclear Engineering and Design* 1985; **88**:169–178.
29. Hwang H, Jaw JW. Probabilistic damage analysis of structures. *Journal of Structural Engineering* 1990; **116**:1992–2007.
30. Dutta A. On energy based seismic analysis and design of highway bridges. *Ph.D. Thesis*, State University of New York at Buffalo, 1999.

31. Fang JQ, Li QS, Jeary AP, Liu DK. Damping of tall buildings: its evaluation and probabilistic characteristics. *Structural Design of Tall Buildings* 1999; **8**:145–153.
32. Bavarisetty R, Vinayagamoorthy M, Duan L. Dynamic analysis. In *Bridge Engineering Handbook*, Chen W-F, Duan L (eds). CRC Press: Boca Raton, FL, 2000.
33. Nielson B, DesRoches R. Effect of using PGA versus Sa on the uncertainty in probabilistic seismic demand models of highway bridges. *8th National Conference on Earthquake Engineering*, Earthquake Engineering Research Institute, San Francisco, 2006.
34. FEMA. *HAZUS-MH MRI: Technical Manual*, Federal Emergency Management Agency, Washington, DC, 2003.
35. Padgett JE, DesRoches R. Bridge damage-functionality using expert opinion survey. *8th National Conference on Earthquake Engineering*, Earthquake Engineering Research Institute, San Francisco, 2006.
36. Mosleh A, Apostolakis G. The assessment of probability distributions from expert opinions with an application to seismic fragility curves. *Risk Analysis* 1986; **6**:447–461.